

## Phonon Lasing from Optical Frequency Comb Illumination of Trapped Ions

Michael Ip,<sup>1,\*</sup> Anthony Ransford,<sup>1</sup> Andrew M. Jayich,<sup>2</sup> Xueping Long,<sup>1</sup> Conrad Roman,<sup>1</sup> and Wesley C. Campbell<sup>1</sup>

<sup>1</sup>*Department of Physics and Astronomy, University of California, Los Angeles, Los Angeles, California 90095, USA*

<sup>2</sup>*Department of Physics, University of California, Santa Barbara, Santa Barbara, California 93106, USA*



(Received 6 December 2017; published 25 July 2018)

We demonstrate the use of a frequency-doubled optical frequency comb to load, cool, and crystallize trapped atomic ions as an alternative to ultraviolet (UV) or even deep UV continuous-wave lasers. We find that the Doppler shift from the atom's oscillation in the trap, driven by the blue-detuned comb teeth, introduces additional cooling and amplification which gives rise to steady-state phonon lasing of the ion's harmonic motion in the trap. The phonon laser's gain saturation keeps the optical frequency comb from continually adding energy without bound. This protection allows us to demonstrate loading and crystallization of hot ions directly with the comb, eliminating the need for a continuous-wave cooling laser, a technique that is extendable to the deep UV.

DOI: 10.1103/PhysRevLett.121.043201

Valence electrons in ions are tightly bound, typically requiring laser light in the ultraviolet (UV) for Doppler cooling [1–4]. This is particularly problematic for species requiring light at wavelengths shorter than  $\lambda \approx 204$  nm [5], which include  $\text{Hg}^+$  [6,7],  $\text{Al}^+$  [8,9],  $\text{He}^+$  [10,11], and highly charged ions [12]. While continuous-wave (cw) laser light is challenging to produce in the UV and deep UV, mode-locked (ML) lasers can be converted to short wavelengths due to their high instantaneous intensity [13,14], providing an attractive alternative for working with ions. We find that in addition to Doppler cooling with a single mode of the frequency comb, interaction with multiple modes gives rise to phonon lasing [15], allowing for the study of higher order oscillation amplitudes in a single ion system that is explained with a simple model.

The promise of appreciable coherent optical power at challenging wavelengths has driven research in optical frequency comb laser cooling [16–19]. The two demonstrated approaches for ions relied on ultraviolet cw lasers to load and precool the ions before introducing the comb, whereas this work shows that only the UV comb is required. In the “broadband laser” regime [16] (where the excited state lifetime is shorter than the pulse repetition period,  $\tau < T_r$ ), Doppler cooling was performed by positioning the laser's center frequency to the red side of resonance. We show that even in this regime, significant comb tooth effects persist that can explain the observed anomalously low temperatures. In another approach [18], motional amplification by blue-detuned teeth was avoided by using a high-repetition-rate ( $1/T_r = 373$  MHz) laser. The frequency comb in that work was unable to crystallize initially hot ions, and several improvements were suggested for achieving this goal, including further shortening the repetition period of the laser [18].

In this Letter, we show that multitooth effects protect the ion from unbounded motional amplification and permit

loading, cooling, and crystallization of hot ions directly with standard frequency combs, eliminating the need for UV cw lasers. By using a frequency comb that is able to achieve intensities per tooth of order  $I_{\text{sat}}$  (50 mW/cm<sup>2</sup> for a typical ion cycling transition), we are able to observe and manipulate the ion's behavior even when it is not cooled to crystallization. Instead of heating the ion out of the trap, we find that multiple comb teeth give rise to stable phonon lasing of the ion's motion [15,20], an interpretation that is confirmed by injection locking the ion's amplified mechanical oscillation [21]. Irrespective of the sign of detuning for the comb tooth closest to resonance, saturable vibrational lasing leads to a comb of stable, fixed-point oscillation amplitudes maintained by cooperative effects between red- (cooling) and blue-detuned (amplifying) comb teeth. We find that ions in high-amplitude fixed points can be probabilistically transferred to lower amplitude fixed points by scanning the detuning, thereby allowing them to be cooled into the lowest fixed point and crystallized. We also present a theoretical model of this behavior that agrees with our observations, and provide an expression for the achievable Doppler limit for laser cooling with optical frequency combs.

Single  $^{174}\text{Yb}^+$  (or  $^{171}\text{Yb}^+$ ) ions for this work are confined in a radio-frequency (rf) Paul trap with oblate spheroidal symmetry [22], driven by a sinusoidal voltage at  $\Omega_{\text{rf}} = 2\pi \times 48.535$  MHz. The secular frequencies of motion are typically  $(\omega_x, \omega_y, \omega_z) \approx 2\pi \times (550, 500, 920)$  kHz ( $\pm 2\pi \times 10$  kHz) where the trap axis of symmetry is along the  $z$  direction. We illuminate the ions with laser beams that are confined to the  $xy$  plane and  $\omega_x$  is the frequency of the phonon mode that lases most frequently due to the fact that it is closest to parallel to the ML laser propagation direction ( $\Delta\theta = 23^\circ \pm 2^\circ$ , see Fig. 1). Fluorescence emitted in the

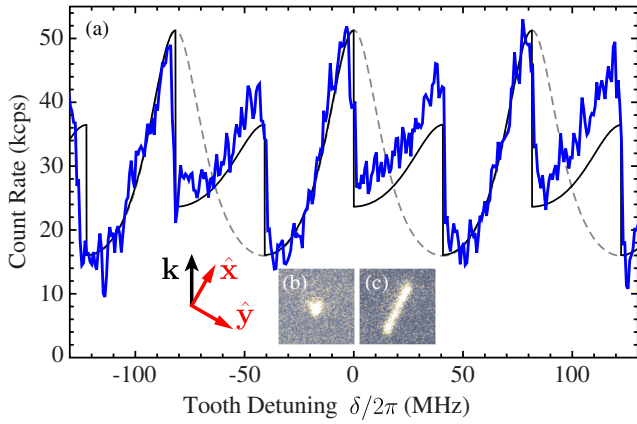


FIG. 1. Fluorescence spectrum (in kilocounts per second) from a single trapped ion illuminated by an optical frequency comb. When the near-resonant tooth is red detuned, the ion is localized via Doppler cooling (b) and the spectrum (a) follows the rest-frame line shape from Eq. (1) (dashed, gray). When the near-resonant tooth is blue detuned, the ion oscillates with a fixed amplitude (c) and the fluorescence shows clear departure from the natural rest-frame resonance shape. The solid black curve is  $\Gamma(\delta, x_0)$  with oscillation amplitude  $x_0 = 0$  or  $x_0 = 4.9 \mu\text{m}$  when the near-resonant comb tooth is red or blue detuned, respectively. The systematic increase in count rate from left to right is consistent with laser intensity drifts during the measurement.

-z direction is collected by an imaging system and recorded on a photon-counting photomultiplier tube (PMT) and intensified CCD camera through a 369 nm bandpass filter.

The ML laser for this work is a commercial picosecond Ti:sapphire laser oscillator [23] with a repetition rate of  $f_r = 1/T_r = 81.553 \text{ MHz}$ . The center frequency of the laser is set near 405.645 THz, and the output is frequency doubled via a single pass through a 0.8 cm LBO crystal cut for type I phase matching for SHG of 760 nm light, generating an average UV power of around 9 mW at  $\lambda \approx 369.5 \text{ nm}$ . The laser bandwidth ( $> 10 \text{ GHz}$ ) far exceeds the natural linewidth ( $\gamma \equiv 1/\tau = 2\pi \times 19.7 \text{ MHz}$ ) and Zeeman splitting ( $< 5 \text{ MHz}$ ) of the  $^2P_{1/2} \leftrightarrow ^2S_{1/2}$  transition in  $\text{Yb}^+$ . The peak ion fluorescence observed indicates that the optical power per comb tooth at the ion is  $\approx 1.4 \mu\text{W}$ . For all of the experiments reported here, we simultaneously illuminate the trapped ion with the mode-locked laser at 369.5 nm and a cw repump laser at 935 nm that has no observable direct mechanical effect on the ion.

The quasi-steady-state scattering rate for an atom at rest illuminated by a resonant comb of uniformly intense teeth ( $\tau_{\text{pulse}} \ll T_r$ ) is given by [24–26]

$$\Gamma_{\text{comb}}(\delta) = \frac{1}{T_r} \frac{\sin^2(\frac{\theta}{2}) \sinh(\frac{\gamma T_r}{2})}{\cosh(\frac{\gamma T_r}{2}) - \cos^2(\frac{\theta}{2}) \cos(\delta T_r)}, \quad (1)$$

where  $\delta$  is the angular detuning of a reference tooth from resonance ( $\delta \equiv \omega_{\text{tooth}} - \omega_{\text{atom}}$ ) and  $\theta$  is the pulse area,

defined as the integral of the instantaneous Rabi frequency for a single pulse,  $\theta \equiv \int dt \Omega(t)$ .

We quantify the relative importance of considering a comblike vs broadband (single-pulse) spectrum by the tooth visibility  $V \equiv (\Gamma_{\text{max}} - \Gamma_{\text{min}})/(\Gamma_{\text{max}} + \Gamma_{\text{min}})$ . From Eq. (1), we find

$$V = \cos^2\left(\frac{\theta}{2}\right) \text{sech}\left(\frac{\gamma T_r}{2}\right), \quad (2)$$

which shows that phase-coherent, interpulse effects persist far into the  $\tau < T_r$  regime, tracking the decay of the off-diagonal elements of the density matrix (i.e., the coherences) more closely than the populations. For instance, the lifetime-limited ( $\theta \rightarrow 0$ ) tooth visibility in this work is  $V = 0.77$  despite  $\sim 78\%$  of the excited state population decaying between pulses.

Figure 1(a) shows the 369.5 nm fluorescence collected from a trapped ion as the teeth of the frequency comb illuminating it are scanned. The dashed gray curve is from Eq. (1), and has been adjusted for the overall vertical scale (with no offset) and is shown for  $\theta = 0.38\pi$ , yielding a measured tooth visibility of  $V = 0.53$ . The data are taken for 100 ms of illumination per point so that the motional temperature reaches steady state for each frequency shown. Background counts ( $\approx 170 \text{ kcps}$ ) have been subtracted by taking the difference between the signal with and without the 935 nm repump laser.

The fluorescence in Fig. 1(a) tracks the ion’s power-broadened rest-frame line shape well when the near-resonant tooth is on the red side of atomic resonance ( $\delta < 0$ ). As the near-resonant tooth crosses resonance and becomes blue detuned ( $\delta > 0$ ), the fluorescence no longer follows the rest-frame prediction of Eq. (1), and an additional peak appears. As shown in Fig. 1(c), the ion in this case oscillates with a large amplitude [ $x_0 = (4.9 \pm 0.5) \mu\text{m}$ ].

We model the fluorescence spectrum of a slowly oscillating ion ( $\omega_x \ll \gamma$ ) with secular amplitude  $x_0$  by calculating the average scattering rate over a secular trap period ( $T_{\text{sec}} \equiv 2\pi/\omega_x$ ):  $\Gamma(\delta, x_0) \equiv \langle \Gamma_{\text{comb}} \rangle_{T_{\text{sec}}}$  [27].

The black curve in Fig. 1 shows the model’s predicted scattering rate (scaled for the overall signal height) with a constant oscillation amplitude of  $x_0 = 4.9 \mu\text{m}$  when the nearest-resonant tooth is on the blue side of resonance and  $x_0 = 0$  on the red side. The asymmetric extra peak appearing blue of resonance is due to the shape of the cycle-averaged spectrum (which has a micromotion sideband at  $+\Omega_{\text{rf}}$ , see Supplemental Material [27]) and the abrupt transition to a localized ion when the near-resonant tooth switches between blue and red detuning.

The ion’s large amplitude oscillations are due to a nonlinear, multitooth effect. A trapped ion illuminated by two colors of cw laser light (one red- and the other blue-detuned) can be mapped onto a van der Pol oscillator [15,21,28], a prototypical, self-sustained oscillator model

that can arise in the description of optical lasers [29]. The blue-detuned cw laser light can drive stimulated emission of phonons, and its experimental observation was reported as a phonon laser [15].

To model this system, we work with secular-cycle-averaged expressions for the secular energy  $E \equiv \frac{1}{2}m\omega_x^2 x_0^2$ , damping coefficient  $\beta(E)$ , and stochastic heating rate  $S(E)$  from spontaneous emission and the randomness in absorption. The rate of energy transfer from the optical comb to the ion's motion is given by

$$\frac{dE}{dt} = -\beta(E)\frac{2E}{m} + S(E). \quad (3)$$

The stochastic heating power can be calculated from the cycle-averaged scattering rate,  $S(E) = (1 + \zeta)(\hbar^2|\mathbf{k}|^2/2m)\Gamma(\delta, x_0)$ , where  $\zeta = \frac{2}{5}$  is the geometric factor for dipole emission [30] and  $x_0 = \sqrt{2E/m\omega_x^2}$ . The coherent (i.e., nonstochastic) amplification power is given by  $-\beta 2E/m = \langle \mathbf{F} \cdot \mathbf{v}_{\text{sec}} \rangle_{T_{\text{sec}}}$ , where  $\mathbf{F} = \hbar\mathbf{k}\Gamma_{\text{comb}}$  and  $\mathbf{v}_{\text{sec}}(t)$  is the instantaneous secular velocity [27].

In the small oscillation limit ( $E \rightarrow 0$ ), if the comb tooth closest to resonance is red detuned, the amplification factor becomes a damping term (i.e.,  $\beta > 0$ ) and it can Doppler cool the ion's motion much like a single cw laser, as shown in Fig. 1(b). The small amplitude limit of Eq. (3) with  $\mathbf{k}$  along  $\hat{\mathbf{x}}$  yields the frequency comb Doppler cooling limit [31]

$$T_D = \frac{\hbar}{2k_B T_r} (1 + \zeta) \left( \frac{\cosh(\frac{\zeta T_r}{2})}{\cos^2(\frac{\theta}{2}) \sin(\delta T_r)} - \cot(\delta T_r) \right), \quad (4)$$

where  $\delta < 0$ . The minimum temperature is reached at a detuning of

$$\delta_{\text{opt}} = -\frac{1}{T_r} \arccos\left(\frac{\cos^2(\frac{\theta}{2})}{\cosh(\frac{\zeta T_r}{2})}\right). \quad (5)$$

For the parameters in this work, Eq. (4) predicts a temperature of  $T_D = 830 \mu\text{K}$ , less than a factor of 2 higher than the cw Doppler limit predicted for the same saturation parameter ( $T_{D,\text{cw}} = 530 \mu\text{K}$ ). This frequency comb Doppler limit corresponds to a rms displacement of  $x_{\text{rms}} = 60 \text{ nm}$  for  $\delta = -\pi/2T_r$ . Since this is much smaller than the resolution ( $\approx 1 \mu\text{m}$ ) of our imaging system, the images can only be used to place an upper limit of 240 mK on the ion's temperature in this regime. Previous work, however, has confirmed that an ion cooled by a single, red-detuned tooth was cooled to within a factor of 2 of the cw Doppler limit [18].

When the near-resonant comb tooth is on the blue side of the atomic resonance ( $\delta > 0$ ), for small oscillation amplitude there is net gain for the ion's motion from the laser field ( $\beta < 0$ ). This amplification has recently been observed

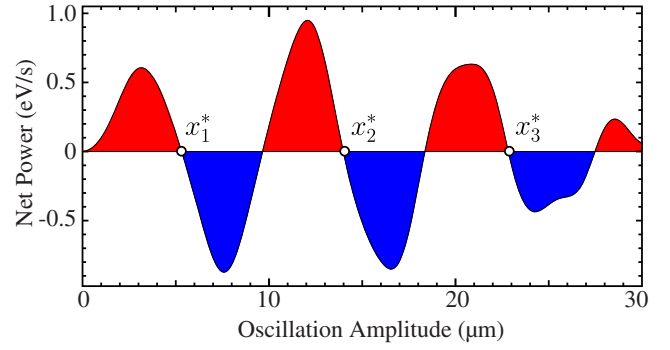


FIG. 2. Calculated net power delivered to the motion of a trapped  $\text{Yb}^+$  atom illuminated by an optical frequency comb as a function of the amplitude of the oscillations in the trap. The right side of Eq. (3) is plotted for the case where the near-resonant tooth is blue detuned with  $\delta = \pi/2T_r$ . Red (blue) shading indicates amplification (damping) of the ion's motion. Stable fixed points are shown by circles. The red-detuned case ( $\delta \rightarrow -\delta$ ) is similar but inverted with an additional fixed point near zero ( $x_0^* = 90 \text{ nm}$ ).

spectroscopically as a line pulling mechanism [32]. Figure 2 shows  $dE/dt$  calculated from Eq. (3) for this case. The frequency comb will add energy to the motion of an initially cold ion until the net power transfer vanishes, leading to a steady-state oscillation that can occur with significant amplitude, as shown in Fig. 1(c). Vanishing net power transfer occurs when the ion's motion induces a Doppler shift large enough to bring a red-detuned tooth into resonance to counteract the amplification with cooling. While we have included the effects of micromotion in our quantitative model (see Refs. [27,33]), the phonon lasing in this case is not induced by the micromotion sidebands (in contrast to Ref. [20]), and the elimination of that effect from our model gives essentially the same predictions with slightly less agreement between theory and the data.

In fact, since the optical frequency comb has many teeth, multiple roots of the right side of Eq. (3) exist for both signs of  $\delta$  (see, e.g., Fig. 2). Those roots with a negative derivative with respect to  $E$  are stable fixed points of the nonlinear differential equation (3), denoted here with a \* (see Fig. 2) [34]. Since both the cooling and heating rates are proportional to the scattering rate, the existence and position of the fixed points of this theory persist even in the limit of low optical intensity, and there is no threshold for this behavior in the absence of additional heating mechanisms. Experimentally, we find that if  $\delta$  changes sign, a new fixed point is reached that is approximately equally likely to be lower or higher in amplitude. By scanning  $\delta$ , we can regularly load and crystallize ions (including multi-ion crystals) with only the ML laser and the 935 nm repump. Applying our model to the parameters in Ref. [18] yields a predicted amplitude of  $\approx 400 \mu\text{m}$  for the lowest blue-detuned fixed point under those conditions. However, these oscillations would have been difficult to observe for two

reasons: the laser spot size ( $\approx 10 \mu\text{m}$ ) would have illuminated only a small fraction of this oscillation amplitude, and for the low scattering rate ( $\approx 1/10$  the value in this work) the fluorescence signal would likely have been below the noise floor.

Figure 3 shows the experimental signature of multiple fixed point solutions for the oscillation amplitude when the near-resonant tooth is red (upper) or blue (lower) detuned. These integrated (along  $\hat{y}$ ) fluorescence images resemble the “two-lobe” shape of a classical harmonic oscillator (or coherent state) probability distribution. The fits, shown as black curves (which include convolution with our imaging system point-spread function), are used to extract the oscillation amplitude fixed points with a resolution-limited systematic uncertainty of  $\pm 0.5 \mu\text{m}$ . When the near-resonant tooth is red detuned, we find stable oscillation amplitudes  $(x_1^*, x_2^*, x_3^*) = (8.6, 16.9, 25.0) \mu\text{m}$ , compared to the theoretical prediction of  $(9.5, 18.0, 27.0) \mu\text{m}$  from the roots of Eq. (3). For the blue-detuned case, we find  $(x_1^*, x_2^*, x_3^*) = (4.9, 12.7, 20.7) \mu\text{m}$ , with the corresponding predicted values  $(5.2, 13.7, 22.4) \mu\text{m}$  (see Fig. 2). The measured fixed points agree with the predicted values to about 10%.

We further verified that the system behaves as a phonon laser amplifier by acoustically injection locking each of the first three fixed points (other than the  $x_0^* \approx 0$  fixed point for  $\delta < 0$ ) for both signs of  $\delta$  using the technique described in Ref. [21], shown in Fig. 4. Injection-locked phonon lasers

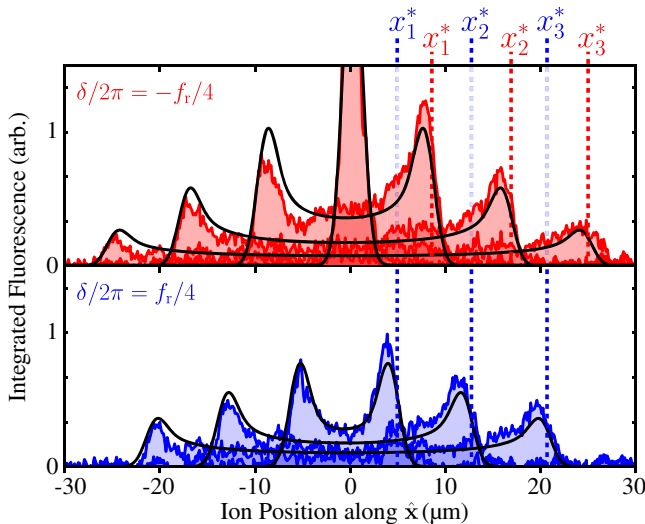


FIG. 3. Integrated ion fluorescence images when illuminated by an optical frequency comb whose nearest-resonant tooth is red detuned (upper) or blue detuned (lower) of rest-frame resonance. Hysteresis associated with the ion’s initial energy determines which fixed point the ion finds. The dashed lines indicate the fixed-point oscillation amplitudes extracted from fitting to classical harmonic oscillator distributions (solid black curves). The systematic fluorescence asymmetry is due to the intensity gradient of the ML laser beam.

of this sort may prove useful as sensitive force sensors [21] or test systems for models of quantum synchronization [28,35,36].

Both the theoretical model and the observed behavior we report show that phenomena arising from interpulse coherence can dominate ML-illuminated ion dynamics in the regime where  $\tau < T_r$ . For the  $\text{Cd}^+$  laser cooling described in Ref. [16], the probability of excited state decay between consecutive pulses was  $P_{\text{decay}}(\gamma, T_r) > 98\%$ , but Eq. (2) shows that the limit on tooth visibility imposed by this decay is nonetheless  $V = 0.27$ , and our model predicts stable fixed points with the lowest lying between 2 mK and 2 K in  $E/k_B$ . Single-pulse cooling effects can be added to our model by including an additional damping coefficient  $\beta_{\text{env}} \approx -(\hbar k/T_r)\partial_v P_{\text{ex}}(\theta, kv)$  due to the slope of the single-pulse excitation probability envelope  $P_{\text{ex}}(\theta, kv)$  to Eq. (3), along with any technical heating rates, and solving for the steady-state energy. As an estimate, for the lowest fixed point and in the absence of any technical heating, the pulse duration for which single-pulse cooling effects are comparable to comb effects will be near  $\tau_{\text{pulse}} \approx 2T_r V \approx 4\cos^2(\theta/2)T_r e^{-\gamma T_r/2}$ .

Since blue-detuned comb teeth do not pose an intractable problem for working with trapped ions, optical frequency combs may prove to be useful and robust tools for a variety of currently difficult species. In the case of  $\text{He}^+$ , which is an attractive spectroscopic subject [10], 1 mW frequency comb light sources may soon become available at  $\lambda \approx 61 \text{ nm}$  [14], and 2-photon transitions could be used for slow Doppler cooling in the limit of low intensity [19]. Direct comb cooling of helium ions may then enable work with  $^3\text{He}^+$ , the lightest atomic cation with an electron (and therefore the most difficult to sympathetically cool with another ion), where the ground state hyperfine splitting of

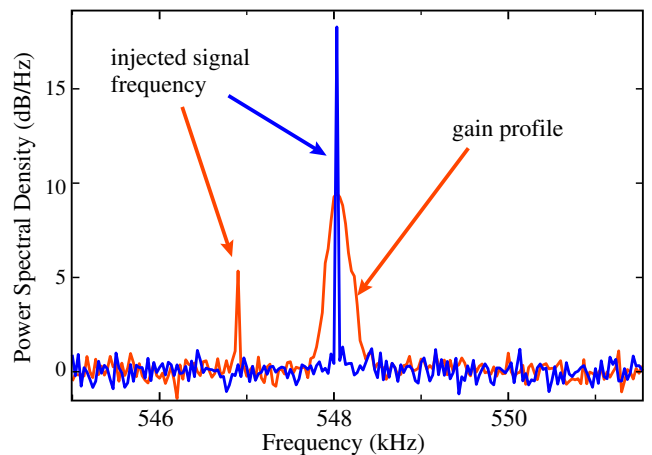


FIG. 4. Acoustic injection locking of the  $x_1^*$  fixed point phonon laser when the near-resonant tooth is blue detuned. When the frequency of an injected signal is moved from outside (orange) to within (blue) the phonon laser’s gain bandwidth, it is amplified at the expense of other frequencies.

8.67 GHz [37] would easily be spanned by a comb for repumping and spectroscopy. We have tested one possible hyperfine repumping scheme for  $I = 1/2$  experimentally by laser cooling and repumping  $^{171}\text{Yb}^+$  with only the ML laser, similar to the case recently reported for  $^{25}\text{Mg}^+$  [18].

The authors acknowledge discussions with Alex Levine and Boris Blinov and thank Eric Hudson for comments on the manuscript. Technical assistance was provided by Sylvi Haendel and Danilo Dadic. This work was supported by the U.S. Army Research Office under Grant No. W911NF-15-1-0261. Initial work by A. M. J. and X. L. was supported by the NSF CAREER Program under Grant No. 1455357.

M. I. and A. R. contributed equally to this work.

\*michaelip9228@physics.ucla.edu

- [1] D. J. Wineland and H. Dehmelt, *Bull. Am. Phys. Soc.* **20**, 637 (1975).
- [2] T. W. Hänsch and A. L. Schawlow, *Opt. Commun.* **13**, 68 (1975).
- [3] W. Neuhauser, M. Hohenstatt, P. Toschek, and H. Dehmelt, *Phys. Rev. Lett.* **41**, 233 (1978).
- [4] D. J. Wineland, R. E. Drullinger, and F. L. Walls, *Phys. Rev. Lett.* **40**, 1639 (1978).
- [5] K. Kato, *IEEE J. Quant. Electr.* **QE-22**, 1013 (1986).
- [6] W. H. Oskay, S. A. Diddams, E. A. Donley, T. M. Fortier, T. P. Heavner, L. Hollberg, W. M. Itano, S. R. Jefferts, M. J. Delaney, K. Kim, F. Levi, T. E. Parker, and J. C. Bergquist, *Phys. Rev. Lett.* **97**, 020801 (2006).
- [7] T. Rosenband, D. B. Hume, P. O. Schmidt, C. W. Chou, A. Brusch, L. Lorini, W. H. Oskay, R. E. Drullinger, T. M. Fortier, J. E. Stalnaker, S. A. Diddams, W. C. Swann, N. R. Newbury, W. M. Itano, D. J. Wineland, and J. C. Bergquist, *Science* **319**, 1808 (2008).
- [8] P. O. Schmidt, T. Rosenband, C. Langer, W. M. Itano, J. C. Bergquist, and D. J. Wineland, *Science* **309**, 749 (2005).
- [9] S.-B. Dai, N. Zong, F. Yang, S.-J. Zhang, Z.-M. Wang, F.-F. Zhang, W. Tu, L.-Q. Shang, L.-J. Liu, X.-Y. Wang, J.-Y. Zhang, D.-F. Cui, Q.-J. Peng, R.-K. Li, C.-T. Chen, and Z.-Y. Xu, *Opt. Lett.* **40**, 3268 (2015).
- [10] M. Herrmann, M. Haas, U. D. Jentschura, F. Kottmann, D. Leibfried, G. Saathoff, C. Gohle, A. Ozawa, V. Batteiger, S. Knünz, N. Kolachevsky, H. A. Schüssler, T. W. Hänsch, and T. Udem, *Phys. Rev. A* **79**, 052505 (2009).
- [11] A. Cingöz, D. C. Yost, T. K. Allison, A. Ruehl, M. E. Fermann, I. Hartl, and J. Ye, *Nature (London)* **482**, 68 (2012).
- [12] J. Nauta, A. Borodin, H. A. Ledwa, J. Stark, M. Schwarz, L. Schmöger, P. Micke, J. R. C. López-Urrutia, and T. Pfeifer, *Nucl. Instrum. Methods Phys. Res., Sect. B* **408**, 285 (2017).
- [13] A. McPherson, G. Gibson, H. Jara, U. Johann, T. S. Luk, I. A. McIntyre, K. Boyer, and C. K. Rhodes, *J. Opt. Soc. Am. B* **4**, 595 (1987).
- [14] G. Porat, C. M. Heyl, S. B. Schoun, C. Benko, N. Dörre, K. L. Corwin, and J. Ye, [arXiv:1710.04314](https://arxiv.org/abs/1710.04314).
- [15] K. Vahala, M. Herrmann, S. Knünz, V. Batteiger, G. Saathoff, T. W. Hänsch, and T. Udem, *Nat. Phys.* **5**, 682 (2009).
- [16] B. B. Blinov, J. R. N. Kohn, M. J. Madsen, P. Maunz, D. L. Moehring, and C. Monroe, *J. Opt. Soc. Am. B* **23**, 1170 (2006).
- [17] D. Kielpinski, *Phys. Rev. A* **73**, 063407 (2006).
- [18] J. Davila-Rodriguez, A. Ozawa, T. W. Hänsch, and T. Udem, *Phys. Rev. Lett.* **116**, 043002 (2016).
- [19] A. M. Jayich, X. Long, and W. C. Campbell, *Phys. Rev. X* **6**, 041004 (2016).
- [20] Y. Xie, W. Wan, H. Y. Wu, F. Zhou, L. Chen, and M. Feng, *Phys. Rev. A* **87**, 053402 (2013).
- [21] S. Knünz, M. Herrmann, V. Batteiger, G. Saathoff, T. W. Hänsch, K. Vahala, and T. Udem, *Phys. Rev. Lett.* **105**, 013004 (2010).
- [22] B. Yoshimura, M. Stork, D. Dadic, W. C. Campbell, and J. K. Freericks, *EPJ Quantum Techno.* **2**, 2 (2015).
- [23] SpectraPhysics Tsunami picosecond ML laser pumped with 10 W cw light at 532 nm.
- [24] D. Felinto, C. A. C. Bosco, L. H. Acioli, and S. S. Vianna, *Opt. Commun.* **215**, 69 (2003).
- [25] E. Ilinova, M. Ahmad, and A. Derevianko, *Phys. Rev. A* **84**, 033421 (2011).
- [26] D. Aumiler and T. Ban, *Phys. Rev. A* **85**, 063412 (2012).
- [27] See Supplemental Material at <http://link.aps.org/supplemental/10.1103/PhysRevLett.121.043201> for expressions of computing cycle averages and a brief discussion of the dependence of fixed points on comb tooth detuning.
- [28] T. E. Lee and H. R. Sadeghpour, *Phys. Rev. Lett.* **111**, 234101 (2013).
- [29] A. Yariv and W. M. Caton, *IEEE J. Quantum Electron.* **10**, 509 (1974).
- [30] D. Leibfried, R. Blatt, C. Monroe, and D. Wineland, *Rev. Mod. Phys.* **75**, 281 (2003).
- [31] The expressions for the comb cooling Doppler limit and the detuning that achieves the minimum temperature remain valid for an atom (whether neutral or ionized) in free space illuminated by a counterpropagating comb-based optical molasses, assuming the relative phase between the two beams is randomized by atomic motion. These expressions reduce to the well-known formulas for cw laser cooling [30] in the limit  $T_r \rightarrow 0$  with  $\theta^2 = s_o T_r^2 \gamma^2 / 2$ .
- [32] A. Ozawa, J. Davila-Rodriguez, J. R. Bounds, H. A. Schuessler, T. W. Hänsch, and T. Udem, *Nat. Commun.* **8**, 44 (2017).
- [33] R. Blümel, C. Kappler, W. Quint, and H. Walther, *Phys. Rev. A* **40**, 808 (1989).
- [34] S. H. Strogatz, *Nonlinear Dynamics and Chaos* (Westview Press, Boulder, CO, 1994).
- [35] T. E. Lee, C.-K. Chan, and S. Wang, *Phys. Rev. E* **89**, 022913 (2014).
- [36] M. R. Hush, W. Li, S. Genway, I. Lesanovsky, and A. D. Armour, *Phys. Rev. A* **91**, 061401 (2015).
- [37] H. A. Schuessler, E. N. Fortson, and H. G. Dehmelt, *Phys. Rev.* **187**, 5 (1969).